

## An elementary survey on structural, electrical, and optical properties of perovskite materials

Bijayalaxmi Kuanar<sup>1)</sup>, Hari S. Mohanty<sup>1)</sup>, Dhrubananda Behera<sup>2)</sup>, Priyambada Nayak<sup>3)</sup> and Biswajit Dalai\*<sup>1)</sup>

<sup>1)</sup>Department of Physics, School of Sciences, GIET University, Gunupur, Rayagada, Odisha-765022, India

<sup>2)</sup>Department of Physics and Astronomy, National Institute of Technology, Rourkela, Odisha-769008, India

<sup>3)</sup>Indian Institute of Technology Bhubaneswar, Odisha-769008, India

Received 13 April 2021

Revised 12 July 2021

Accepted 22 July 2021

### Abstract

The paper is aimed to study the recent progress on lead-free piezoelectric materials, focusing on synthesis and various properties such as structural, electrical and optical of them. Lead zirconate titanate ( $\text{Pb}(\text{Zr}_x\text{Ti}_{1-x})\text{O}_3$ , PZT) and its associated solid solutions are extensively used in several memory devices, sensors, actuators, and transducers in this era. The toxic nature of lead (or lead oxide) creates health and environmental problems. With the environmental concerns, researchers are very much interested in finding out environmental-friendly lead-free materials, which can substitute the said toxic materials with the same industrial applications with high-efficiency situations. Various classes of materials are now under investigation by several researchers, considered as highly potential alternatives to the above said toxic materials. The perovskite structures such as pure Bismuth Sodium Titanate (BNT), its binary and ternary solid solution systems along with their structural, electrical, and optical properties are reviewed in this paper. The observation reveals that various lead-free material compositions illustrate stability in piezoelectric results, even if it is not matching completely with the performance of lead-based material. It motivates active research on this subject matter, i.e., lead-free materials to overcome lead-based materials, cited herewith. This has stimulated us to analyze the function of lead-free material with a vision that it would provide further ignition for a wide range of industrial applications to modern scientists, continuing research in this field.

**Keywords:** PZT, Lead-free, BNT, Dielectric, Ferroelectric properties

### 1. Introduction

From the literature survey, researchers are focusing on the application of high dielectric constant capacitors, buzzers, sensors, ultrasonic motors, actuators, piezoelectric sonar, ultrasonic transducers, medical diagnostic transducers, ferroelectric thin films memories, multilayer capacitors, ferroelectric random-access memory (FERAM), etc. [1-7]. In the past several years, piezoceramic PZT used in functional devices, dominating in industrial applications [8, 9]. But these are toxic due to the presence of lead, which has been proved to be a cause for various health hazards and environmental pollutions [10-14]. However, at present researchers are diverted towards lead-free piezoelectric ceramics, *viz* titanate-based perovskite material ( $\text{BaTiO}_3$ ,  $\text{Na}_{0.5}\text{Bi}_{0.5}\text{TiO}_3$ ,  $\text{K}_{0.5}\text{Bi}_{0.5}\text{TiO}_3$  and  $\text{BaZr}_{0.08}\text{Ti}_{0.92}\text{O}_3$ ), and its solid solutions, the alkaline niobate perovskite ( $\text{KNbO}_3$  and  $\text{NaNbO}_3$ ), and the bismuth-based perovskite materials ( $\text{BiFeO}_3$  and  $\text{BiScO}_3$ ) to find same characteristics in various applications to substitute the lead-based materials [15-22].

In 1880, pressure electricity i.e., piezoelectricity was revealed for the first time by Jacques Curie and Nobel laureates Pierre during the analysis of the effects of presence on the generation of electric charges by a case study in Rochelle salt, tourmaline, and quartz. The chronological listing of many piezo and ferroelectric materials is discovered by Gene. H. Haertling [23, 24]. The piezoelectric effect is the development of an electrical charge on applying mechanical pressure and vice versa. The main drawback of natural piezoelectric materials is the truncated piezoelectricity. Extensively owned and widely exploited piezoelectric materials sensed in 1950 are PZT,  $\text{BaTiO}_3$ , and its family materials those exhibit extreme dielectric as well as piezoelectric properties. However, lead oxide is a PZT component and highly toxic in behavior. The toxicity can be enhanced because of its volatility at a high temperature especially during the sintering and calcination and causes pollution in the environment [24-26]. In recent years, researchers are investigating to substitute the PZT materials to protect the environment. However, continuous research is going on to build up different lead-free materials, for eco-friendly applications [27, 28].

Between the two different lead-free systems: (i) Perovskite materials are Bismuth Sodium Titanate (BNT), Barium Titanate Oxide ( $\text{BaTiO}_3$ ), Potassium Niobate ( $\text{KNbO}_3$ ), Sodium Titanate Oxide ( $\text{NaTiO}_3$ ), etc. [29] (ii) Non-Perovskite materials such as Bismuth layer structure and Tungsten-Bronze are appeared as a suitable material for the substitution of the lead-based ceramics because of high polarization and piezoelectric coefficients [30]. However, the main bottleneck includes low Curie temperature ( $T_C$ ) and high coercive field that make the ceramic strenuous for polarization state transition with remarkable conductivity and dielectric loss [31]. Hence, different approaches have been developed by researchers to overcome these problems, such as high-quality ceramic oxides synthesis, worthy doping at various sites, and solid solution fabrication. Increasing demand for environmental protection, the plethora of

\*Corresponding author. Tel.: +9168 5725 0170

Email address: biswajit@giet.edu

doi: 10.14456/easr.2022.30

investigations on lead-free piezoelectric ceramics is being performed for environmental-friendly applications. Due to the large remnant polarization ( $Pr \sim 38 \mu\text{C}/\text{cm}^2$ ), Bismuth sodium titanate ( $\text{Ba}_{0.5}\text{Na}_{0.5}\text{TiO}_3$ ; BNT) is assumed as a righteous candidate of lead-free piezoelectric ceramics at room temperature. BNT holds a complex perovskite structure and rhombohedral phase. If the transition temperature is  $200^\circ\text{C}$ , it changes to the anti-ferroelectric phase. The Curie temperature ( $T_c$ ) of such material is about  $320^\circ\text{C}$  [32]. Because of the above advantages of BNT, authors mainly focused on the changes in the transition of phases, electrical and dielectric behaviors of BNT, its solid solutions with other perovskite structures, and doping of di, tri, and tetravalent ions at A and/or B-site.

## 2. Experimental details

The sample stoichiometric followed by various research groups [20-26] is displayed in Figure 1. Out of various powder preparation methods available, most commonly the mixed oxide route is followed where appropriate stoichiometric proportions of desired oxides are used. For effective preparation of the mixture, we may traditionally go for the agate motor or ball milling. To achieve the required chemical and optical homogeneity, ball milling is crucial. Proper care shall be taken to ensure the mixture is neither over milled nor under milled because in either case, we may not get the desired mixture. Milling time is based on powder characteristics and varies from 2 hrs to 16 hrs. Generally, the mixtures are milled with either zirconia or alumina balls with non-flammable liquid-like trichloroethylene or distilled water. Excluding those traditional solid-state reaction methods, lead-free piezoelectric materials are produced through several chemical routes like co-precipitation, wet chemical route, and sol-gel, etc. The milled powders then dried and are calcined ( $800^\circ\text{C}$ - $900^\circ\text{C}$ ) for 2 to 3 hrs. During calcination, volatile components like moisture are separated and then the required phase formation occurs. Sometimes the dry powders are re-milled for 4 to 5 hrs with an additional organic vehicle of 20-40 wt %. The organic vehicle generally includes a binder (ethyl cellulose), a plasticizer (polyethylene glycol), a dispersing agent (butoxy ethoxy ethyl acetate), and a solvent ( $\alpha$ -terpineol). The sample density is computed by the Archimedes principle. Sample phase and crystal structure are identified by analyzing X-ray diffraction (XRD). The surface morphology of the sample is inspected with the use of scanning electron microscopy (SEM) and field emission scanning electron microscopy (FESEM). The electron probe approach is used to calibrate the content of an element in a sample. After the calcination process, polyvinyl alcohol (PVA) is used as a binder to press the granulated powder pellets. The pellets are then sintered at a temperature varying between  $1050^\circ\text{C}$ - $1200^\circ\text{C}$ . For electrode, the sintered pellets are coated with silver paste and for orientation, the ferroelectric domains in ceramic and electrical properties are measured by applying a strong DC field.

Dielectric measurement (dielectric loss and dielectric constant) was performed with the use of an automatic LCR Meter Bridge. A Sawyer-Tower circuit is used to perform ferroelectric hysteresis measurement. A constant tester of the piezoelectric is used to measure the piezoelectric coefficient  $d_{33}$ . The other properties of materials are studied by using Raman, FTIR, PL, and UV by the researchers [22-25] for various industrial applications.

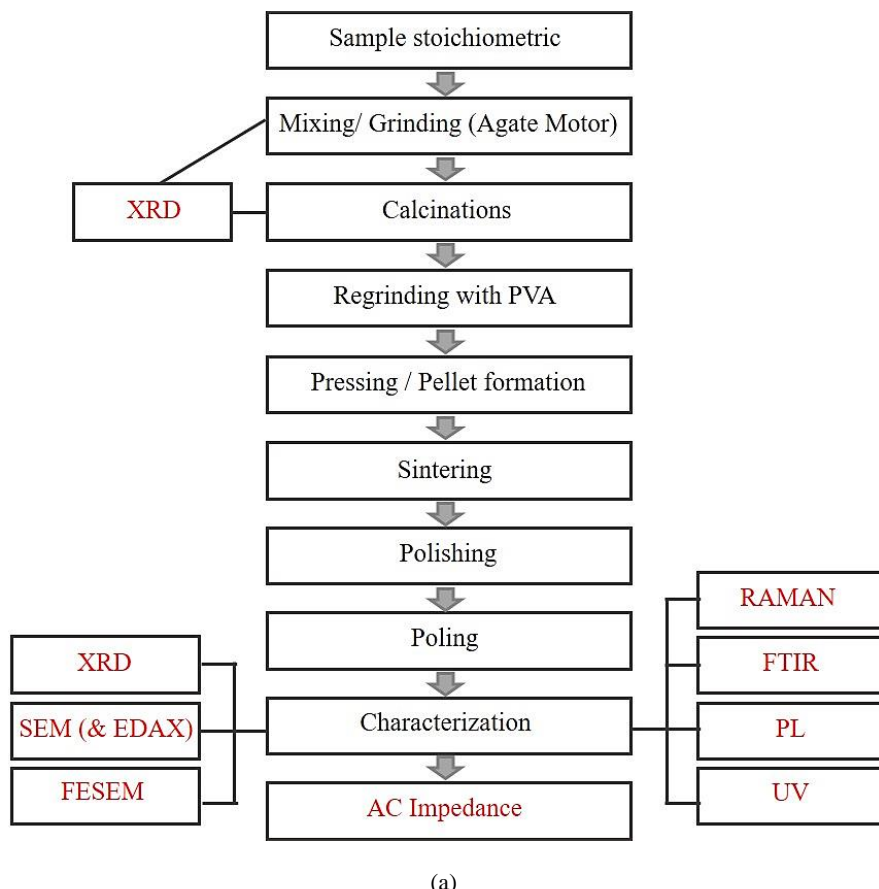
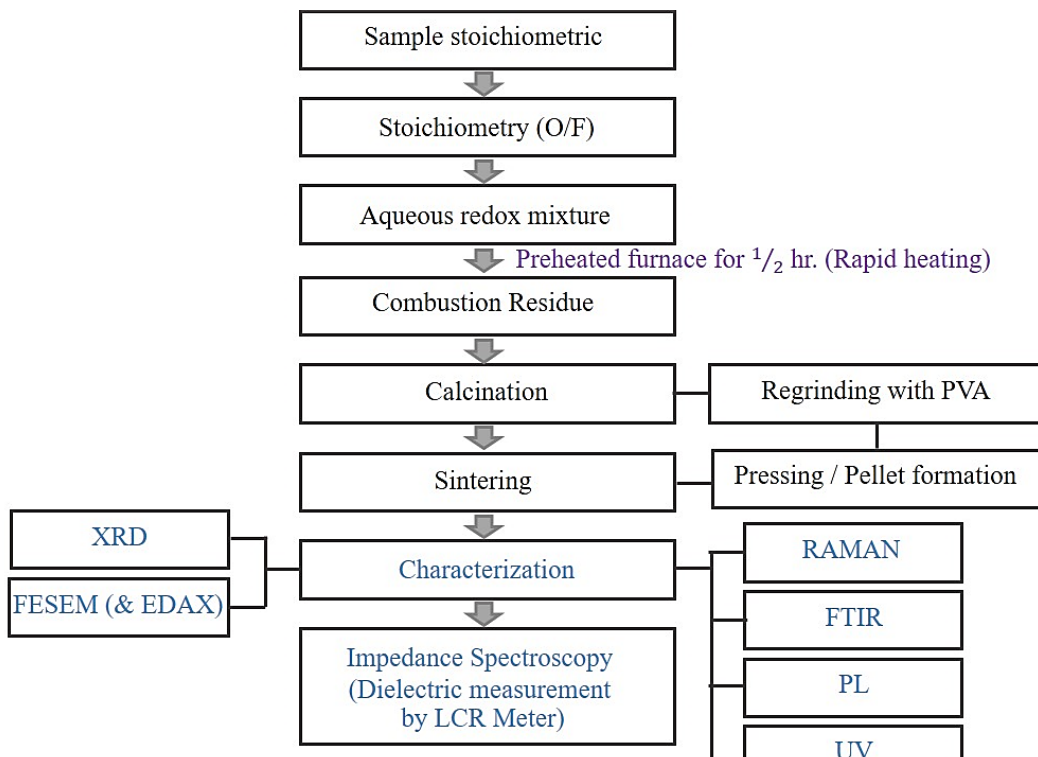
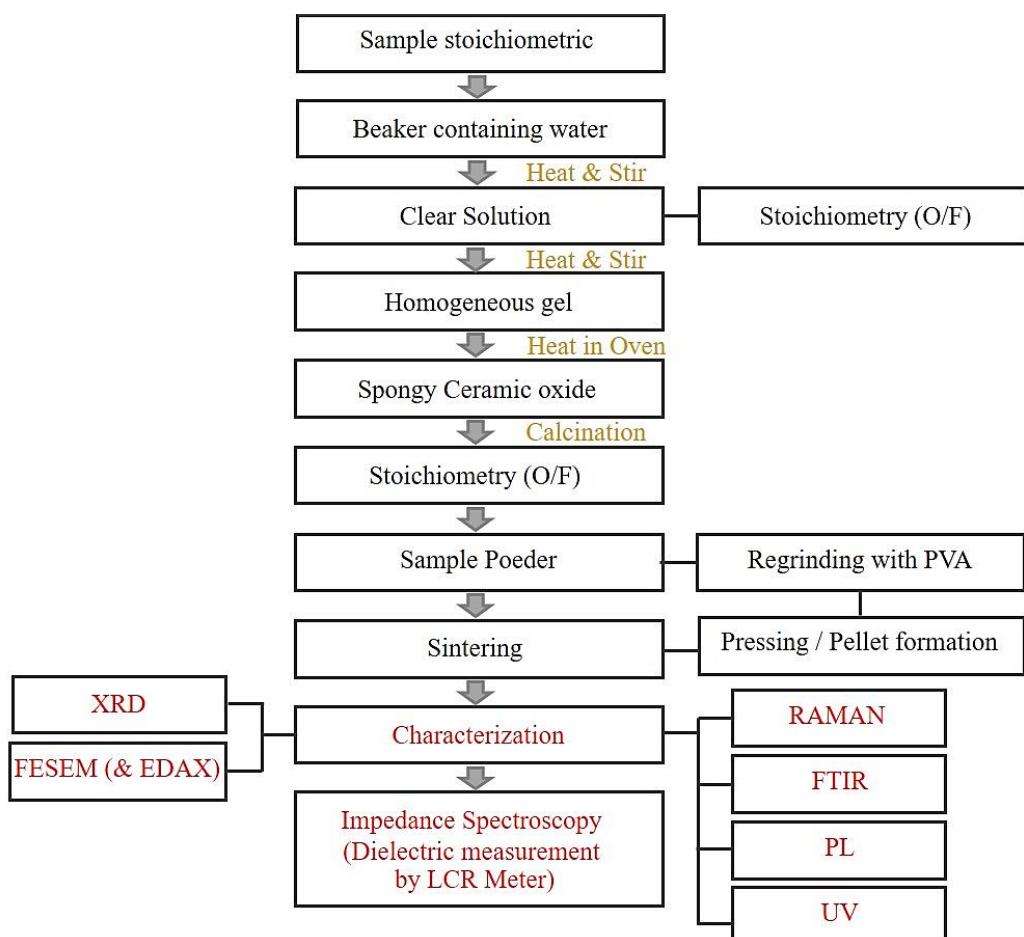


**Figure 1** Steps for sample preparation and characterization: (a) Solid-state route, (b) Auto-combustion route and (c) Sol-gel route.



(b)



(c)

**Figure 1** (continued) Steps for sample preparation and characterization: (a) Solid-state route, (b) Auto-combustion route and (c) Sol-gel route.

### 3. Results and discussion

#### 3.1 Bismuth sodium titanate and related materials

The ferroelectric oxides with general formula  $ABO_3$ , considered as a perovskite structure, such as  $Bi_{0.5}Na_{0.5}TiO_3$ (BNT),  $BaTiO_3$ (BT),  $KNbO_3$ ,  $NaTiO_3$ ,  $NaTaO_3$ , etc. are the renowned lead-free piezoelectric materials. The physical properties of such structure are tuned easily with the use of several iso- and aliovalent substitutions either at A site or B site of  $ABO_3$  structure as per the requirement of its simple structure. Sodium bismuth titanate ( $Bi_{0.5}Na_{0.5}TiO_3$ ) is a righteous material among the lead-free ceramics due to its high remnant polarization ( $P_r=38 \mu C/cm^2$ ), strong ferroelectricity property, high Curie temperature ( $T_c=320 ^\circ C$ ), and moderate piezoelectric constant ( $d_{33}=73 \text{ pC/N}$ ) [33, 34]. However, the coercive field ( $E_c=73 \text{ kV/cm}$ ) makes poling difficult which restricts the application. For reducing leakage current, enhanced piezoelectric constant, decrease coercive field, remnant polarization, and depolarization temperature, several substitutions, dopant, and cations are added to BNT. It is observed that for BNT ceramic, modification in B-site is less effective than A-site due to the cations ordering of  $Bi^{3+}$  and  $Na^{1+}$  [35-39]. Hence, it is concluded from the above-mentioned review that the good piezoelectric property is achieved with partial substitution of the rare earth element (+3) valence state either by A-site or B-site individually into the BNT ceramics system. The donor doping (more positive ion) and acceptor dopant (lower valence ion) for  $ABO_3$  perovskite structure, induces and reduces A-site vacancies respectively. It also promotes the vacancies of oxygen in the A-site for maintaining overall charge neutrality in the lattice [40]. A-site vacancies formation in the donor dopant system is used to promote the wall motion domain and improve ferroelectric behavior. However, in the acceptor doped system, the free oxygen vacancies restrict it by pinning of the domain walls. The group theory of Raman active phonon modes for rhombohedral (R3C) phase are presented by 4A1 (IR, R) +9E (IR, R) of optical IR and Raman modes [41]. The Raman scattering modes in BNT material are the result of relaxor-based perovskite ferroelectric material characteristics. Researchers pointed out the low-frequency regions ( $100-200 \text{ cm}^{-1}$ ) dominations due to the displacement of Bi-O and Na-O; more specifically these modes are extensively sensitive to atomic mass vibration instead of bond length. The B-site cation vibrations cause mid-frequency regions ( $200-400 \text{ cm}^{-1}$ ) like Ti-O bond and the high-frequency regions ( $450-700 \text{ cm}^{-1}$ ) [42]. However, higher frequency regions ( $700-950 \text{ cm}^{-1}$ ) are assigned to oxygen atom vibrations.

#### 3.2 Addition of dopants with BNT and their effects

It has been observed that BNT based compositions modified with  $BaTiO_3$ ,  $BiKTiO_3$ ,  $NaNbO_3$ ,  $BiFeO_3$ ,  $La_2O_3$ ,  $Sc_2O_3$ ,  $BaCO_3$  etc [43-49] showed improved properties and are easy to be poled.

##### 3.2.1 Effect of Zr

The substitution of Zr in the B-site enhances the relative ionic displacement and electrical property by the expansion of the perovskite lattice. It can also be seen that with the substitution of Zr suppresses the conduction in electronic hoping in an oxidation state of  $Ti^{4+}$  and  $Ti^{3+}$ .  $Zr^{4+}$  can be seen as a preservative, which results decrease in the dielectric constant ( $\epsilon_r$ ) and stable leakage current [50]. In the modified sample the grain size has increased. They studied that observance of phase transition at a higher frequency, tangent loss increment with increasing temperature for 1MHz frequency have been seen. Furthermore, the loss tangent of the Zr modified BNT sample was too small till  $300 ^\circ C$ , and a sudden hike in this value above this. The A.C conductivity was calculated by using the formula of  $\sigma_{ac} (= \epsilon_0 \epsilon_r \omega \tan\delta)$ . An increment in dielectric constant is observed with increasing temperature up to the maximum value ( $\epsilon_{max}$ ) then decrement.

##### 3.2.2 Effect of Gd doped sodium bismuth titanate

Behara et al. [51] reported the optical, structural, and Raman studies of Gd doped Bismuth sodium titanate ( $Gd_xNBT$ ) system. The addition of Gd at the Bi site shows distortion and it's an amphoteric dopant. The authors also demonstrated that for  $x=0.08$  the bandgap is the lowest ( $E_g=2.78 \text{ eV}$ ). Therefore, there was a possibility of using this material as a photo-voltaic cell.

##### 3.2.3 Effect of MgO

Bismuth magnesium titanate ( $Bi (Mg_{0.5}Ti_{0.5}) O_3$ ) [BMT] is a rhombohedral ferroelectric perovskite similar to sodium bismuth titanate ( $Bi_{0.5}Na_{0.5}TiO_3$  [BNT] ceramics. For improving ferroelectric and piezoelectric property Ruth et al. [52] have studied the Mg dopant's effects as an additive. It is being concluded that Rhombohedral structure is maintained till  $x=0.04$ -mole fraction and it changed to cubic phase in higher mole fraction. The shape of the grain might be changed as a reason of size difference in different. Dielectric loss and dielectric constant decrease with frequency. In BMT substituted samples remnant polarization ( $P_r$ ) and saturation polarization ( $P_s$ ) are enhanced and coercive field is reduced up to  $x=0.04$ . From the Raman effect, it was studied that for the frequency range of  $109-134 \text{ cm}^{-1}$  dominated by Bismuth-Oxide vibration,  $155-187 \text{ cm}^{-1}$  dominated by Na-O vibration, and  $246-401 \text{ cm}^{-1}$  dominated by  $TiO_6$  vibration.

##### 3.2.4 Study of BNT-Bi, BNT-Na, BNT-BT and BNT-SBT system

Piezoelectric and Thermal depoling properties of Bismuth Sodium Titanate ceramic were investigated with a new group of compounds ( $Bi_{0.5}Na_{0.5}TiO_3$ - $(Bi_{0.5}(1+x)Na_{0.5})TiO_3-0.75x$ ) by Hiruma et al. [53]. The ratios of assumed and measured densities were more than 97 %. With the increase in Bi or decrease in Na in BNT the resistivity increases and it is highest at BNT-Na (-0.01) i.e.,  $\rho=4.15 \times 10^{13} \Omega$ . Because of the high value of conductivity and pinning domains, it is difficult to pole in the BNT ceramics. The single-phase of complex structured rhombohedral symmetry was marked and confirmed in the X-ray diffraction. The dielectric loss lowered in BNT when Na/Bi ratio is greater than 1.0 and the highest depolarization temperature of pure BNT, BNT-Bi (0.01), BNT-Na (-0.01), BNT-Na (-0.02) was  $187 ^\circ C$ ,  $181 ^\circ C$ ,  $185 ^\circ C$ , and  $172 ^\circ C$  respectively. Furthermore, the leakage current increases above  $T_d$  (depolarization temperature) because of high conductivity. It has also been reported that BNT ceramic exhibits three depoling processes that occur at the interval of  $T_d$ ,  $T_d$  to  $T_{R-T}$ , and  $T_{R-T}$  to  $T_m$ . Another interesting BNT based ceramic (1-x) NBT-xBT was studied by Mohanty et al.

[29]. The authors have reported the transition of structural phase using XRD and Raman spectra with intermediate coexistence of the morphotropic phase boundary (MPB). All the ferroelectric and dielectric properties are enlisted in Table 1.

**Table 1** Properties of NBT-BT system

Compositions (1-x) NBT-xBT	$T_m$ (°C)	$T_{FR}$ (°C)	$\tan\delta$	$\epsilon_r$	$P_r$ ( $\mu\text{C}/\text{cm}^2$ )	$E_c$ (kV/cm)
$x = 0.00$	335	170	0.01389	2100	71.8	58.6
$x = 0.02$	315	160	0.00571	2500	46.7	48.2
$x = 0.05$	305	137	0.01229	3800	15.4	34.7
$x = 0.06$	290	105	0.0355	4800	57.7	28.8
$x = 0.07$	270	109	0.04749	4100	37.1	22.1
$x = 0.08$	260	120	0.06313	2900	17.1	22.4
$x = 0.10$	255	133	0.0193	2400	13.94	22.6

Hajar et al. [54] elaborately studied the influence of a small amount of (2.0 wt. %) of  $\text{Ba}^{2+}$  ions on A and B- site substitution in BNT. They analyzed the transition of phases, relaxor properties, and electrical properties of the modified (BNT-BT) material. They also reported that with the increase in frequency there was a rapid decrease in the dielectric constant and arrives at a saturation limit above 10 kHz. The dielectric loss reduces with the increasing frequency too. The non-ohmic type of conduction behavior was obtained from J-E characteristics. So, they anticipated that, because of low dielectric loss and porosity, it could be a low loss material. Further, the ferroelectric relaxor can facilitate reducing the polarization. Wang et al. [55] reported the strain hysteresis. The highest piezoelectric coefficient ( $d_{33}$ ) of 1658 pC/N and large electrostrictive coefficient  $Q = 0.287 \text{ m}^4\text{C}^2$  were obtained in the ceramics of (1-x)  $\text{Bi}_{0.5}\text{Na}_{0.5}\text{TiO}_3$ -x  $\text{Sr}_{0.85}\text{Bi}_{0.1}\text{TiO}_3$  sintered at 1260 °C and most importantly the P-E loops were hysteresis-free, indicate a suitable material for high-precision actuator application. When x is closed to 0.06-0.08 [4], the presence of MPB is revealed in Figure 2 reflecting binary system phase (1-x)  $\text{Bi}_{1/2}\text{Na}_{1/2}\text{TiO}_3$ - x  $\text{BaTiO}_3$  (BNT-BT). Based on the enhanced property of piezoelectric, MPB existence becomes evident at this composition.

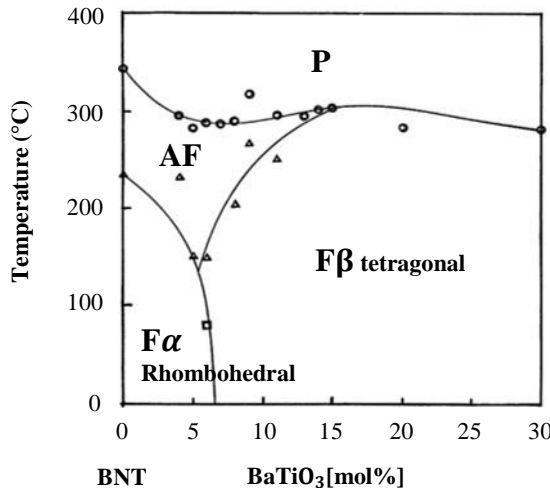


**Figure 2** Morphotropic Phase boundaries in BNT-BT.

### 3.2.5 Effect of $\text{K}_2\text{CO}_3$ and $\text{Nb}_2\text{O}_3$ (KNBN)

Du et al. [56] studied different properties of  $\text{BiNbO}_3$ , such as phase structure, electrical properties, and microstructure for industrial application with A and B-site doping with the chemical formula  $(\text{K}_{0.5}\text{Na}_{0.5})_{1-3x}\text{BiNbO}_3$ . It was concluded that for  $x \leq 0.01$  orthorhombic phase was maintained at room temperature. The orthorhombic cubic phase with intermediate tetragonal phase was obtained at 174 °C to 403 °C respectively. Temperature-dependent dielectric permittivity was flat up to 170 °C for  $x = 0.01$ . It has been observed that pure BNT ceramics suffers from two bottlenecks i.e. lower phase transition and higher coercive field. By adding only, a 0.01-mole fraction of KNBN, the grain boundary was cleared, no pores were observed. The authors were also studied that the piezoelectric coefficient can be increased and coercive field can be decreased by adding  $\text{Bi}^{3+}$ , at  $x = 0.01$ . It is observed that the  $d_{33}=164 \text{ pC/N}$ ,  $Q_m=120$ ,  $K_p=0.47$ ,  $P_r = 30.1 \mu\text{C}/\text{cm}^2$ ,  $T_c = 403 \text{ }^\circ\text{C}$ , and lastly  $E_c = 6.18 \text{ kV/cm}$  which confirms that the material can be a suitable candidate for industrial application. Again, an excess of 0.8 mol. % of  $\text{K}_2\text{CO}_3$  repays the potassium loss as a reason for its volatility. The  $d_{33}$  value of the NKBT20 [57] sample was found to be 215 pC/N. The values of the coercive field and remnant polarization are 39 kV/cm and 56.7  $\mu\text{C}/\text{cm}^2$  respectively.

### 3.2.6 Effect of $\text{BaZrO}_3$

Lead-free ferroelectric ceramics  $[0.94(\text{Bi}_{0.5}\text{Na}_{0.5}\text{TiO}_3-0.06\text{BaTiO}_3)]-x\text{BaZrO}_3$  (abbreviated as BNBT-XBZ) are considered as righteous candidates for the actuator devices [58]. The authors reported about the strain hysteresis decreases with the increase of the applied electric field. The X-ray diffraction (XRD) reports prove the transformation of crystal structure transforms from a mixed phase of rhombohedral and tetragonal mixed to tetragonal phase with the growth of BZ doping. Destruction of ferroelectricity with BZ concentration growth is signified in P-E and J-E loops. They also reported that out of all other concentrations BNBT-0.03BZ outperforms in strain behavior. The hysteresis value and strain decrease with the increasing amount of BZ.

### 3.2.7 The effect of $BaTiO_3$

The importance of flexoelectricity in a solid material is recently being observed. The solid-phase method with working formula  $(Na_{0.5}Bi_{0.5})_{1-x}Ba_xTiO_3$  where  $x$  value is in the range (0.0, 0.02, 0.04, 0.06, 0.08 and 0.10) is used for preparing the  $NBBT_x$  ceramic [59]. Due to various thermal contractions in between reduced and unreduced layers a curve structure is formed. Flexoelectricity is a coupling between orientational deformation and electric polarization in the ferroelectric material. The content of 6 mol. % of  $BaTiO_3$  in the above said sample has the highest value of  $d_{33}=120$  pC/N. The values of dielectric constant and loss are 787 and 0.0709 respectively. The authors have compared the change in piezoelectric, ferroelectric, and dielectric properties of the reduced sample  $NBBT-6$  before and after polarization as follows: (i) The unpolarised sample show better ferroelectricity and the piezoelectric constant of the modified sample ( $d_{33}=108.7$  pC/N), (ii) post-polarization piezoelectric coefficient of modified sample increased to 133 pC/N. post-reduction dielectric constant and loss decrease to 693 and 0.0909 respectively and (iii) post-reduction remnant polarization and displacement of polar strain increase to  $21.84 \mu C/cm^2$  and 2590 nm respectively. However, the coercive field was reduced to 1.88 kV/cm from 2.35 kV/cm. Sahoo et al. [60] prepared  $0.92(Bi_{0.5}Na_{0.5}TiO_3) + 0.08(BaTiO_3)$  abbreviated as (BNT-BT8) ceramic by conventional solid-state reaction route. Raman and FTIR spectra identified the vibrational as well as the phonon modes of molecular structure. They concluded that adding a smaller amount of Barium Titanate in material causes an increase in dielectric constant and a fall in the tangent loss. The strong dependency of electrical parameters on frequency and temperature is shown by impedance spectroscopy. The increment in dielectric property can make energy storage devices suitable. Yang et al. [61] doped  $Ta^{5+}$  with  $BaTiO_3$ -BNT and studied the room-temperature resistivity of the prepared samples ( $x=0.005$ ). They found that the resistivity decreased first and then increased with the increase of  $x$ . At  $x = 0.003$ , the room-temperature resistivity reached the minimum. The  $T_c$  values of all samples were enhanced, and then decreased with doping content of  $Ta^{5+}$ , and at  $x= 0.001$ , the sample had the highest value of  $T_c$  up to  $170^{\circ}C$ . The authors in [62] have marked the intrinsic and extrinsic electric response in (BNT-xBT) ceramic. The morphotropic phase boundaries (MPB) between rhombohedral and tetragonal exists in the range of  $x= 0.06-0.08$ . Their findings illustrate that piezoelectric coefficient  $d_{33}$  of 151 pC/N and electrochemical coupling factor  $k_p$  of 0.278 were obtained for the ceramic with  $x$  value 0.07 near the MPB region. Cernea et al. [63] also studied various properties of BNT-BT ( $x= 0.08$ ) thin film, such as optical, electrical, and structural properties which were processed by sol-gel route. It is observed that the dielectric constant  $\epsilon_r$  and loss tangent are 243 and 0.38 respectively. They also reported the value of remnant polarization  $P_r$  as  $0.87 \mu C/cm^2$ .

### 3.2.8 BNT- $SrNb_2O_6$ ceramic

With the use of substitution at A and B-site, BNT ceramics properties are being modified. Controlling of dopants on phase transitions, piezoelectric coefficients, relaxor behavior, and electromechanical properties is also being reported. Bajpai and his co-workers [64] in this work further studied the relaxor behaviour and dielectric relaxation in  $(1-x)(Bi_{0.5}Na_{0.5}TiO_3)-x(SrNb_2O_6)$  (BNT-SN) where the  $x$  value can be 0.01, 0.02 and 0.03. They observed that the temperature-dependent dielectric property shows a broad dielectric curve for BNT-SN solid solutions. It shows frequency-dependent shifts towards higher temperatures, which confirms typical relaxor behavior. Furthermore, the diffuseness increases from 73 to 95 with the increasing content of SN (for  $x = 0.01, 0.02$  and 0.03). Mobile cations disorder causes an increment in ionic conductivity. It is considered a major cause of additional dielectric dispersion in the loss spectrum.

### 3.2.9 Effect of lanthanum (La) substitution BNBT ceramics

Anem et al. [65] investigated the effect of La on BNBT7 ceramics. They observed that the single-phase perovskite structure for all dense samples ( $x= 0.0, 0.02, 0.04, 0.06, 0.08$  and 0.10). A thick microstructure with increased grain size has been developed when a small amount of La was added. The dielectric constant increases to the maximum and then fall with an increase in temperature. From the P-E loop, the dielectric loss and porosity show that the materials are low loss in natural material and relaxor in type. The piezoelectric constant  $d_{33}=152$  pm/V and 147 pm/V, coercive field  $E_c=14.78$  kV/cm and 9.24 kV/cm piezoelectric voltage constant  $g_{33}=14.36$  and  $13.37(10^{-3})$  mV/N was found for the composition BNBT-7 and lanthanum substituted BNBT-7 ( $x= 0.02$ ). Hence, it is considered a suitable candidate for the transducer application. The influence of  $La^{3+}$  and  $Sc^{3+}$  dopant was again studied by Verma and Rout [40]. Their research has indicated the influence of donor ( $La^{3+}$ ) and acceptor dopant ( $Sc^{3+}$ ) on the electrical and structural properties of BNT ceramic. The authors have investigated the frequency-dependent ferro and anti-ferro phase transition and internal biased field influencing the piezoelectric coefficient. For both the dopants they found that there was a structural change for pure BNT rhombohedral to the pseudo-cubic structure. It could be concluded that the cationic vacancies created by donor doping. However, oxygen vacancies are induced by acceptor doping. It is not only stabilizing the polarization but also increases the remnant polarization ( $P_r$ ) value. Maximum  $P_r$  for 3.0 % La- doped and 5.0 % Sc was found to be  $27 \mu C/cm^2$  and  $20 \mu C/cm^2$  respectively. For pure BNT, the Curie temperature raised from  $355^{\circ}C$ . But, in the case of donor doped ( $La^{3+}$ ), it raised to  $365^{\circ}C$ . In acceptor doped ( $Sc^{3+}$ ), the temperature raised to  $370^{\circ}C$  for BNT. An increase in the concentration of La dopant which is a result of a large electrostrictive coefficient  $Q_{11} \sim (0.0122 \% - 0.045 \%)$  causes the bipolar strain to increase. Furthermore, the induced electric field was extended to the maximum value  $S_{max}=0.14\%$  for 3.0 % of La having normalized strain  $d_{33}=209$  pm/V at an applied field of 70 kV/cm. However, at an applied field of 50 kV/cm, the  $S_{max}$  value is 0.13 % for 5.0 % of La having normalized strain  $d_{33}=155$  pm/V.

### 3.2.10 BNT-BKT-KNN system

The growth in dielectric, ferroelectric and piezoelectric properties of BNT-based ceramic is a challenge to modern research works. The ternary BNT-BKT-KNN system has also been widely investigated due to its large piezoelectric properties and high dielectric constant (Figure 3). Sumang et al. [66] reported the coexistence of rhombohedral and tetragonal phases indicating the existence of MPB in the composition and obtained the maximum density of  $5.64 \text{ g/cm}^3$ , the utmost reduction of 16.4 % and most favorable dielectric properties  $\epsilon_r=1460$  and  $\epsilon_{SA}=4081$ . The sample also exhibited good ferroelectric properties  $P_r=125 \mu C/cm^2$  and good piezoelectric behavior  $d_{33}=164$  pC/N. The phase diagram of the BNT-BKT-KNN ternary system has been plotted by Lu YQ et. al. [67].

Sumang et al. did a further investigation on dielectric and ferroelectric properties of BNT-BT-xBZT (with  $0 \leq x \leq 0.10$ ). They synthesized the ceramic by the traditional solid-state reaction method. The authors also confirmed the co-existence of rhombohedral and tetragonal phases for all samples and the tetragonal phase increased with an increasing amount of BZT. In Table 2, the values of dielectric constant ( $\epsilon_r$ ), dielectric loss ( $\tan\delta$ ), phase transition temperature ( $T_{FA}$ ), remnant polarization ( $p_r$ ), and coercive field ( $E_c$ ) are presented [68].

**Table 2** Properties of BNT-BT-xBZT system

Compositions (x) [(0.935-x) BNT-0.065BT-xBZT]	$\epsilon_r$ at $T_{FA}$	$\tan\delta$ at $T_{FA}$	$T_{FA}$	$T_{SA}$	$p_r$ ( $\mu\text{C}/\text{cm}^2$ )	$E_c$ (kV/cm)
x= 0	6820	0.015	148	265	32	30
x= 0.02	6956	0.015	154	268	29	23
x= 0.04	7058	0.011	143	280	24	20
x= 0.06	6913	0.011	181	263	24	26
x= 0.08	7234	0.014	197	259	20	29
x= 0.10	8224	0.014	210	249	21	31

Another report described the role of  $\text{BiFeO}_3$  on the electrical and electrochemical properties as well as structure (microstructure) of the BNT-BKT<sub>x</sub>-BF<sub>y</sub> ternary system [69], presented in Table 3.

The incorporated BF disseminates into the BNT-BKT lattice to come out a solid solution but decreases the tetragonal and rhombohedral distortions with a strong influence on properties concluding as a good piezoelectric material.

**Table 3** Properties of BNT-BKT<sub>x</sub>-BF<sub>y</sub> system

Compositions (x,y)	$\epsilon_r$	$\tan\delta$	$p_r$ ( $\mu\text{C}/\text{cm}^2$ )	$E_c$ (kV/mm)	$d_{33}$ (pC/N)
(0.18, 0)	1344	0.047	33.5	3.20	150
(0.18, 0.03)	1233	0.048	28.9	3.16	125
(0.18, 0.07)	1187	0.052	27.5	2.73	70
(0.20, 0)	1743	0.053	37.5	2.90	195
(0.20, 0.03)	1411	0.053	33	2.36	155
(0.20, 0.07)	1235	0.055	28.9	2.00	120
(0.22, 0)	1518	0.051	34	1.64	160
(0.22, 0.03)	1375	0.054	7.6	0.83	20
(0.22, 0.07)	1274	0.056	5.4	0.78	8

### 3.2.11 BNT -BKT- BT system

Further, enhanced performance was found in the Rb-modified BNT-BKT-BT system. Zhou et al. reported that the multi-component lead-free material [0.85Ba<sub>0.5</sub>Na<sub>0.5</sub>TiO<sub>3</sub>-0.11Bi<sub>0.5</sub>K<sub>0.5</sub>-xRb<sub>x</sub>TiO<sub>3</sub>-0.04BaTiO<sub>3</sub>] exhibited good piezoelectric performance and excellent fatigue resistance [70]. Due to the occupation of Rb on A-site, the relaxor property of the composition is enhanced. The piezoelectricity of 203 pC/N and all most fatigue-free behavior were achieved in the composition with  $x= 0.10$ . Trellcat et al. [71] investigated morphotropic phase boundary in the BNT-BKT-BT system as shown in Figure 3.

With the increase in BKT and BT amount, the value of the dielectric constant increases for all compositions. The ternary mixture, i.e., 0.865 BNT-0.035 BT-0.100 BKT morphotropic composition shows high electromechanical coupling factors ( $k_p = 0.26$  and  $k_t = 0.57$ ) piezoelectric constant ( $d_{33} = 133$  pC/N) which confirm good piezoelectric property [71] and is presented in Table 4.

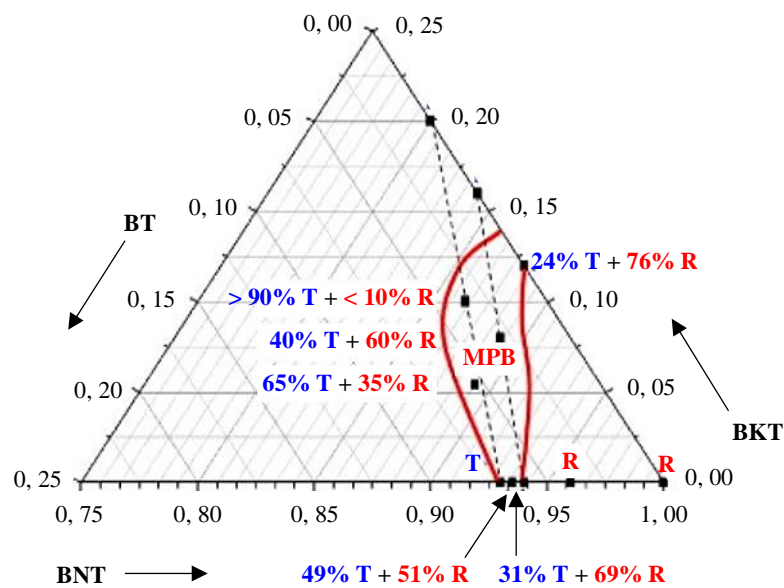


**Figure 3** Morphotropic phase boundary of BNT-BKT-BT System [24].

**Table 4** Properties of BNT-BKT-BT content

Compounds	$\epsilon_r$	$\tan \delta$	$k_p$	$k_t$	$d_{33}$ (pC/N)
BNT	423	5.0	$0.11 \pm 0.01$	$0.49 \pm 0.02$	$67 \pm 10$
0.96 BNT-0.04 BT	532	1.7	$0.13 \pm 0.01$	$0.43 \pm 0.02$	$123 \pm 10$
0.94 BNT-0.06 BT	782	3.1	$0.35 \pm 0.02$	$0.53 \pm 0.05$	$170 \pm 4$
0.935 BNT-0.065 BT	873	3.4	$0.26 \pm 0.01$	$0.49 \pm 0.05$	$147 \pm 9$
0.93 BNT-0.07 BT	626	2.1	$0.18 \pm 0.02$	$0.45 \pm 0.05$	$123 \pm 3$
0.88 BNT-0.12 BKT	541	4.1	$0.22 \pm 0.01$	$0.43 \pm 0.03$	$78 \pm 9$
0.84 BNT-0.16 BKT	710	3.6	$0.29 \pm 0.01$	$0.44 \pm 0.02$	$130 \pm 7$
0.80 BNT-0.20 BKT	936	3.9	$0.39 \pm 0.01$	$0.54 \pm 0.05$	$137 \pm 7$
0.892 BNT-0.054 BT-0.054 BKT	904	3.6	$0.20 \pm 0.02$	$0.43 \pm 0.01$	$130 \pm 10$
0.89 BNT-0.03 BT-0.08 BKT	665	3.8	$0.26 \pm 0.01$	$0.44 \pm 0.02$	$112 \pm 4$
0.865 BNT-0.035 BT-0.100 BKT	891	4.2	$0.26 \pm 0.02$	$0.57 \pm 0.05$	$133 \pm 6$

**Table 5** Properties of some BNT-based solid solution systems

Compositions	$\epsilon_r$	$\tan \delta$ (%)	$d_{33}$ (pC/N)	$K_p$ (%)	$T_c$ (°C)	$T_d$ (°C)	$P_r$ $\mu$ C/cm <sup>2</sup>	Ref.
(1-x) Na <sub>0.5</sub> Bi <sub>0.5</sub> TiO <sub>3</sub> -xBi (Mg <sub>0.5</sub> Ti <sub>0.5</sub> ) O <sub>3</sub>			108					[52]
(Bi <sub>0.5</sub> Na <sub>0.5</sub> ) TiO <sub>3</sub> -(Bi <sub>0.5(1+x)</sub> Na <sub>0.5</sub> ) TiO <sub>3-0.75x</sub>	583		72.9, 81.3 (highest)			187 (highest)		[53]
(1-x) Bi <sub>0.5</sub> Na <sub>0.5</sub> TiO <sub>3</sub> -xSr <sub>0.85</sub> Bi <sub>0.1</sub> TiO <sub>3</sub>			1658					[55]
(K <sub>0.5</sub> Na <sub>0.5</sub> ) <sub>1-3x</sub> BiNbO <sub>3</sub>	750	0.03	164	0.47	403		30.1	[56]
0.8(Na <sub>0.5</sub> Bi <sub>0.5</sub> ) TiO <sub>3</sub> -0.2(K <sub>0.5</sub> Bi <sub>0.5</sub> ) TiO <sub>3</sub>			215				56.7	[57]
NaBiTiZrO <sub>3</sub> (5%Zr)	1618					313		[50]
(Na <sub>0.5</sub> Bi <sub>0.5</sub> ) <sub>1-x</sub> Ba <sub>x</sub> TiO <sub>3</sub> (6 mol%)	787	0.0709	120					[59]
0.92(Bi <sub>0.5</sub> Na <sub>0.5</sub> TiO <sub>3</sub> ) +0.08 (BaTiO <sub>3</sub> )	2573	< 0.1				301		[60]
0.912Ba <sub>0.97</sub> TiO <sub>3</sub> -0.088 (Bi <sub>0.5</sub> Na <sub>0.5</sub> ) TiO <sub>3</sub> -xTa <sub>2</sub> O <sub>5</sub>						170		[61]
0.93(Bi <sub>0.5</sub> Na <sub>0.5</sub> ) TiO <sub>3</sub> -0.07 BaTiO <sub>3</sub>			151	0.278				[62]
[(Bi <sub>0.5</sub> Na <sub>0.5</sub> ) TiO <sub>3</sub> ] <sub>0.92</sub> -[BaTiO <sub>3</sub> ] <sub>0.08</sub>	243						0.87	[63]
(BNT-BT <sub>0.08</sub> )								
Bi <sub>0.465-x</sub> La <sub>x</sub> Na <sub>0.465</sub> Ba <sub>0.07</sub> TiO <sub>3</sub>			152					[65]
(Bi <sub>1-x</sub> La <sub>x</sub> ) <sub>0.5</sub> Na <sub>0.5</sub> TiO <sub>3</sub> (3%La doped)			209		365		27	[40]
Bi <sub>0.5</sub> Na <sub>0.5</sub> (Ti <sub>1-x</sub> Sc <sub>x</sub> ) O <sub>3</sub> (5%Sc doped)			155		370		20	[40]
0.77Bi <sub>0.5</sub> Na <sub>0.5</sub> TiO <sub>3</sub> -0.20 Bi <sub>0.5</sub> K <sub>0.5</sub> TiO <sub>3</sub> -0.03 K <sub>0.5</sub> Na <sub>0.5</sub> NbO <sub>3</sub>	1460		164				125	[66]
0.85Ba <sub>0.5</sub> Na <sub>0.5</sub> TiO <sub>3</sub> -0.11 Bi <sub>0.5</sub> K <sub>0.5</sub> -xRb <sub>x</sub> TiO <sub>3</sub> -0.04 BaTiO <sub>3</sub>			203					[70]
0.9BaTiO <sub>3</sub> -0.1 (Bi <sub>0.5</sub> Na <sub>0.5</sub> ) TiO <sub>3</sub> +NiNb <sub>2</sub> O <sub>6</sub>	1652	1.8				144.9		[72]

### 3.2.12 BT-BNT-NiNb<sub>2</sub>O<sub>6</sub> system

The result of NiNb<sub>2</sub>O<sub>6</sub> content on the dielectric properties and structure of the BT-BNT system was observed [72]. The result shows that doping of NiNb<sub>2</sub>O<sub>6</sub> can suppress grain growth. Initially, the dielectric constant increased at a low temperature then decreased. Curie temperature has been increased slightly with doping concentration. For 1.5 mol.% NiNb<sub>2</sub>O<sub>6</sub> doped specimen, exceptional dielectric properties have been revealed at room temperature with a dielectric constant value 1652 and a dielectric loss value found in different pieces of literature, as mentioned in Table 5.

Perovskite ceramics families become visible to be suitable for piezoelectric and electrostrictive applications. Multi-layered capacitors are such an application of ferroelectric materials [73]. So far, electro-active materials are mostly applied in piezoelectric ceramics. These materials are used in making motors, generators, sonar, sensors, and actuators [74-77]. Some of the piezoelectric materials are being used for making devices operated at high frequencies i.e., resonant devices. A novel application of the materials is sensors, photostrictive actuator, piezoelectric composites (piezoelectric transducers), hydrophones, and medical ultrasonic [78-84]. On the other hand, because of the less transparency, less uniform of the ferroelectric ceramics (polycrystalline) on a microscopic scale suit electro-optic applications widely. Most of the applications are associated with bulk materials. However, trends toward thick and thin films have also been developed for some application. The application of thick films (2-20  $\mu$ m) includes electro-optic and piezoelectric devices [85], whereas, the applications of thin films (0.2-2  $\mu$ m) are infrared sensors memories, capacitors, buffer layers, antireflection coating, and integrated optics [86-88]. Because of the crystallographic asymmetric structure of the piezoelectric materials, they are also extensively used as an energy-harvesting technology. An extensive overview on the applications of piezoelectric materials on bioimplantable energy harvesters is also carried out [89]. In addition to above, piezoelectric nanomaterials (PNs) are also used in nanoprobes, nanosensors, nanoactuators and nanogenerators [90]. As memory becomes more important, transition towards films will become a major requirement in the future. The development of FERAM films for non-volatile memory applications such as smart cards, random access memories of computer and radio frequency identification tags, had already reached modest production levels for specific applications [91-97].

#### 4. Summary

Lead-free ferroelectric ceramic oxides are highly used in modern technology for their high dielectric constant, piezoelectric coefficient, large remnant polarization, low coercive field, and high Curie temperature to substitute the extensively used lead-based ceramics, due to their pollution-free eco-friendly nature. However, these ferroelectric oxides suffer serious polarization problems. Among the perovskite structure of ferroelectric i.e.,  $ABO_3$  type, BNT is considered as an excellent candidate for high  $T_c$  of 320  $^{\circ}\text{C}$ , coercive field,  $E_c$  of 73 kV/cm, and large remnant polarization,  $P_r$  of 38  $\mu\text{C}/\text{cm}^2$ . Due to the large coercive field and high conductivity, PZT is ahead of BNT in industrial applications. For this reason, we intend to develop new lead-free ferroelectric oxides having suitable properties for multi-functional applications in a wide temperature and frequency range. A novel type of application of the materials is the photostrictive actuator which is the combined result of the photovoltaic effect and piezoelectric effect. One of the applications of piezoelectric composites is piezoelectric transducers. These ceramics-polymer composites have a broad range of applications in hydrophones, sensors and, medical ultrasonic. On the other hand, because of the less transparency, less uniform of the ferroelectric ceramics (polycrystalline) on a microscopic scale suit for a variety of electro-optic applications. Therefore, researchers have been investigating many dopants into bismuth sodium titanate ceramics to resolve industrial needs and in the future, it is expected that smart and very smart materials will be developed for a wide range of applications.

#### 5. Acknowledgements

The authors are grateful to the President, Vice President, and Registrar of GIET University for motivation. One of the authors (Bijayalaxmi Kuanar) is thankful to Dr. Dillip Kumar Pattanayak, Associate Professor, Physics, GIET University for fruitful discussions on experimental part of the article.

#### 6. References

- [1] Awan MQ, Ahmad J, Noren L, Lu T, Liu Y. Structure, dielectric and ferroelectric properties of lead free (K, Na)  $(\text{Nb})\text{O}_{3-x}\text{BiErO}_3$  piezoelectric ceramics. *J Mater Sci Mater Electron*. 2018;29(9):7142-51.
- [2] Hussain A, Sinha N, Dhankhar K, Joseph A, Kumar B. Giant piezoelectric behavior in relaxor ferroelectric environment friendly  $\text{Na}_{0.52}\text{K}_{0.44}\text{Li}_{0.04}\text{Nb}_{0.84}\text{Ta}_{0.10}\text{Sb}_{0.06}\text{O}_3$  ceramics for high temperature applications. *J Mater Sci Mater Electron*. 2018;29(8):6403-11.
- [3] Barick BK, Choudhary RN, Pradhan DK. Dielectric and impedance spectroscopy of zirconium modified  $(\text{Na}_{0.5}\text{Bi}_{0.5})\text{TiO}_3$  ceramics. *Ceram Int*. 2013;39(5):5695-04.
- [4] Reichmann K, Feteira A, Li M. Bismuth sodium titanate-based materials for piezoelectric actuators. *Materials*. 2015;8(12):8467-95.
- [5] Li S, Liu J, Guo T, Dong W, Bi K, Luo Y. Piezoelectricity and flexoelectricity of sodium bismuth titanate-based ceramics. *Ceram Int*. 2020;46:2049-54.
- [6] Pal V, Dwivedi RK, Thakur OP. Dielectric and ferroelectric properties of lead-free  $[\text{1}-\{(\text{Bi}_{1-x}\text{La}_x)_{0.5}(\text{Na}_{1-y}\text{Li}_y)_{0.5}\text{TiO}_3\}-z\text{BaTiO}_3]$  ceramic system. *Adv Mater Sci Eng*. 2013;2013:125634.
- [7] Anem S, Rao KS, Rao KH. Investigation of lanthanum substitution in lead-free BNBT ceramics for transducer applications. *Ceram Int*. 2016;42(14):15319-26.
- [8] Okayasu M, Sato Y, Takasu S, Mizuno M, Shiraishi T. Material properties of bismuth layered ferroelectrics and lead zirconate titanate piezoelectric ceramics. *Ceram Int*. 2013;39:3301-6.
- [9] Perumal RN, Athikesavan V, Nair P. Influence of lead titanate additive on the structural and electrical properties of  $\text{Na}_{0.5}\text{Bi}_{0.5}\text{TiO}_3\text{-SrTiO}_3$  piezoelectric ceramics. *Ceram Int*. 2018;44(11):13259-66.
- [10] Babu MVG, Bagyalakshmi B, Giridharan NV, Duraisamy D, Balasubramanian S. Coexistence of ferroelectric phases and electric field induced structural transformation in sodium potassium bismuth titanate ceramics. *J Appl Phys*. 2018;123(3):234101.
- [11] Kornpom C, Chootin S, Bongkarn T. Enhancing piezoelectric of d33 coefficient of new  $(1-x)$  BNKLLT-xNKLNST lead-free ceramics synthesized by the solid state combustion technique. *Integrated Ferroelectrics Int J*. 2017;177(1):121-30.
- [12] Barick BK, Mishra K, Arora A, Choudhary R, Pradhan D. Impedance and Raman spectroscopic studies of  $(\text{Na}_{0.5}\text{Bi}_{0.5})\text{TiO}_3$ . *J Phys Appl Phys*. 2011;44:355402.
- [13] Barick BK, Choudhary R, Pradhan D. Phase transition and electrical properties of lanthanum-modified sodium bismuth titanate. *Mater Chem Phys*. 2012;132:1007.
- [14] Mohanty HS, Dam T, Borkar H, Kumar A, Mishra KK, Sen S, et al. Studies of ferroelectric properties and leakage current behaviour of microwave sintered ferroelectric  $\text{Na}_{0.5}\text{Bi}_{0.5}\text{TiO}_3$  ceramic. *Ferroelectrics*. 2017;517(1):25-33.
- [15] Bajpai KK, Sreenivas K, Gupta AK, Shukla AK. Cr-doped lead lanthanum zirconate titanate (PLZT) ceramics for pyroelectric and energy harvesting device applications. *Ceram Int*. 2019;45(11):14111-20.
- [16] Hiruma Y, Imai Y, Watanabe Y, Nagata H, Takenaka T. Large electrostrain near the phase transition temperature of  $(\text{Bi}_{0.5}\text{Na}_{0.5})\text{TiO}_3\text{-SrTiO}_3$  ferroelectric ceramics. *Appl Phys Lett*. 2008;92(26):262904.
- [17] Zhu Y, Zhou H, Sun D. Bipolar and unipolar fatigue property in  $\text{Bi}_{0.5}\text{Na}_{0.5}\text{TiO}_3\text{-Bi}_{0.5}\text{K}_{0.5}\text{TiO}_3\text{-SrTiO}_3$  lead-free piezoelectric ceramics. *Phys B Condens Matter*. 2019;575:411716.
- [18] Lian HL, Shao XJ, Chen XM. Structure and electrical properties of  $\text{Ca}^{2+}$ -doped  $(\text{Na}_{0.47}\text{Bi}_{0.47}\text{Ba}_{0.06})\text{TiO}_3$  lead-free piezoelectric ceramics. *Ceram Int*. 2018;44(10):11320-30.
- [19] Acosta M, Liu N, Deluca M, Heidt S, Ringl I, Dietz C, et al. Tailoring ergodicity through selective a-site doping in the  $\text{Bi}_{1/2}\text{Na}_{1/2}\text{TiO}_3\text{-Bi}_{1/2}\text{K}_{1/2}\text{TiO}_3$  system. *J Appl Phys*. 2015;117(13):134106.
- [20] Groh C, Jo W, Rodel J. Frequency and temperature dependence of actuating performance of  $\text{Bi}_{1/2}\text{Na}_{1/2}\text{TiO}_3\text{-BaTiO}_3$  based relaxor/ferroelectric composites. *J Appl Phys*. 2014;115(23):234107.
- [21] Cho JH, Jeong YH, Nam JH, Yun JS, Park YJ. Phase transition and piezoelectric properties of lead-free  $(\text{Bi}_{1/2}\text{Na}_{1/2})\text{TiO}_3\text{-BaTiO}_3$  ceramics. *Ceram Int*. 2014;40(6):8419-25.
- [22] Dash SK, Kant S, Dalai B, Swain MD, Swain BB. Characterization and dielectric properties of barium zirconium titanate prepared by solid state reaction and high energy ball milling processes. *Indian J Phys*. 2014;88(2):129-35.
- [23] Haertling GH. Ferroelectric ceramics: history and technology. *J Am Ceram Soc*. 1999;82(4):797-18.

- [24] Panda PK. Environmental friendly lead-free piezoelectric materials. *J Mater sci.* 2009;44:5049-62.
- [25] Lei N, Zhu M, Yang P, Wang L, Wang L, Hou Y, et al. Effect of lattice occupation behavior of  $\text{Li}^+$  cations on microstructure and electrical properties of  $(\text{Bi}_{1/2}\text{Na}_{1/2})\text{TiO}_3$ -based lead-free piezoceramics. *J Appl Phys.* 2011;109(5):054102.
- [26] Xie Z, Gui Z, Li L, Su T, Huang Y. Microwave sintering of lead-based relaxor ferroelectric ceramics. *Mater Lett.* 1998;36(1-4):191-4.
- [27] Badapanda T, Venkatesan S, Panigrahi S, Kumar P. Structure and dielectric properties of bismuth sodium titanate ceramic prepared by auto-combustion technique. *Process Appl Ceram.* 2013;7(3):135-41.
- [28] Szeremeta A, Lazar I, Molak A, Gruszka I, Koperski J, Soszynski A, et al. Improved piezoelectric properties of  $\text{Pb}(\text{Zr}_{0.70}\text{Ti}_{0.30})\text{O}_3$  ceramics doped with non-polar bismuth manganite. *Ceram Int.* 2019;45(15):18363-70.
- [29] Mohanty HS, Dam T, Borkar H, Pradhan DK, Mishra KK, Kumar A, et al. Structural transformations and physical properties of  $(1-x)\text{Na}_{0.5}\text{Bi}_{0.5}\text{TiO}_3-x\text{BaTiO}_3$  solid solutions near a morphotropic phase boundary. *J Phys Condens Matter.* 2018;31(7):075401.
- [30] Du H, Zhou W, Luo F, Zhu D, Qu S, Pei Z. An approach to further improve piezoelectric properties of  $(\text{K}_{0.5}\text{Na}_{0.5})\text{NbO}_3$ -based lead-free ceramics. *Appl Phys Lett.* 2007;91(20):202907.
- [31] Mohanty HS, Kumar A, Sahoo B, Kurliya PK, Pradhan DK. Impedance spectroscopic study on microwave sintered  $(1-x)\text{Na}_{0.5}\text{Bi}_{0.5}\text{TiO}_3-x\text{BaTiO}_3$  ceramics. *J Mater Sci Mater Electron.* 2018;29(8):6966-77.
- [32] Kornphom C, Rittisak J, Laowanidwatana A, Bongkarn T. Enhanced dielectric and ferroelectric behavior in 0.94 BNT-0.06 BCTS lead free piezoelectric ceramics synthesized by the solid state combustion technique. *Integrated Ferroelectrics Int J.* 2018;187(1):20-32.
- [33] Ullah A, Ullah A, Ullah M, Zeb A, Khan Z, Ikram M, et al. Dielectric, ferroelectric, and strain properties of lead-free  $(1-y)\text{BNT}-y\text{ST}$  ceramics. *J Mater Sci Mater Electron.* 2020;31(6):5667-73.
- [34] Cui W, Wang X, Li L. Large piezoelectric properties of  $(1-x)\text{Na}_{0.5}\text{Bi}_{0.5}\text{TiO}_3-x\text{BaTiO}_3$  thin films prepared by sol-gel method. *J Mater Sci Mater Electron.* 2016;27(7):7287-91.
- [35] Razak KA, Song WC, Ng CY. Properties of Ce-doped  $\text{Bi}_{0.5}\text{Na}_{0.5}\text{TiO}_3$  synthesized using the soft combustion method. *Procedia Chem.* 2016;19:816-21.
- [36] Zhao ZH, Ge RF, Dai Y. Large electro-strain signal of the BNT-BT-KNN lead-free piezoelectric ceramics with  $\text{CuO}$  doping. *J Adv Dielectrics.* 2019;9(3):1950022.
- [37] Selvadurai AP, Pazhivelu V, Vasanth BK, Jagadeeshwaran C, Murugaraj R. Investigation of structural and optical spectroscopy of 5% Pr doped  $(\text{Bi}_{0.5}\text{Na}_{0.5})\text{TiO}_3$  ferroelectric ceramics: site depended study. *J Mater Sci Mater Electron.* 2015;26:7655-65.
- [38] Su Lee D, Jong Jeong S, Soo Kim M, Hyuk Koh J. Electric field induced polarization and strain of Bi-based ceramic composites. *J Appl Phys.* 2012;112:124109.
- [39] Huitema L, Cernea M, Crunceanu A, Trupina L, Nedelcu L, Banciu MG, et al. Microwave dielectric properties of BNT-BT<sub>0.08</sub> thin films prepared by sol-gel technique. *J Appl Phys.* 2016;119:144103.
- [40] Verma R, Rout SK. Frequency-dependent ferro-antiferro phase transition and internal bias field influenced piezoelectric response of donor and acceptor doped bismuth sodium titanate ceramics. *J Appl Phys.* 2019;126(9):094103.
- [41] Suchanicz J, Jankowska-Sumara I, Kruzina TV. Raman and infrared spectroscopy of  $\text{Na}_{0.5}\text{Bi}_{0.5}\text{TiO}_3\text{-BaTiO}_3$  ceramics. *J Electroceramics.* 2011;27(2):45-50.
- [42] Hung NT, Bac LH, Hoang NT, Vinh PV, Trung NN, Dung DD. Structural, optical, and magnetic properties of  $\text{SrFeO}_3$ -d-modified  $\text{Bi}_{0.5}\text{Na}_{0.5}\text{TiO}_3$  materials. *Phys B Condens Matter.* 2018;531:75-8.
- [43] Cho JH, Jeong YH, Nam JH, Yun JS, Park YJ. Phase transition and piezoelectric properties of lead-free  $(\text{Bi}_{1/2}\text{Na}_{1/2})\text{TiO}_3\text{-BaTiO}_3$  ceramics. *Ceram Int.* 2014;40(6):8419-25.
- [44] Jan SU, Zeb A, Milne SJ. Electrical properties of Ca-modified  $\text{Na}_{0.5}\text{Bi}_{0.5}\text{TiO}_3\text{-BaTiO}_3$  ceramics. *Ceram Int.* 2014;40(10):15439-45.
- [45] Parija B, Badapanda T, Rout SK, Cavalcante LS, Panigrahi S, Longo E, et al. Morphotropic phase boundary and electrical properties of  $1-x\text{[Bi}_{0.5}\text{Na}_{0.5}\text{]} \text{TiO}_3-x\text{Ba}[\text{Zr}_{0.25}\text{Ti}_{0.75}]\text{O}_3$  lead-free piezoelectric ceramics. *Ceram Int.* 2013;39(5):4877-86.
- [46] Lin D, Kwok KW. Structure and piezoelectric properties of new  $(\text{Bi}_{0.5}\text{Na}_{0.5})_{1-x-y}\text{Ba}_x(\text{Yb}_{0.5}\text{Na}_{0.5})_y\text{TiO}_3$  lead-free ceramics. *J Mater Sci Mater Electron.* 2010;21(11):1119-24.
- [47] Li D, Shen ZY, Li Z, Wang X, Luo WQ, Song F, et al. Structural evolution, dielectric and ferroelectric properties of  $(1-x)\text{Bi}_{0.5}\text{Na}_{0.5}\text{TiO}_3-x\text{Ba}_{0.5}\text{Sr}_{0.5}\text{TiO}_3$  ceramics. *J Mater Sci Mater Electron.* 2019;30(6):5917-22.
- [48] Chen X, He F, Wang Y, Liang F, Zhou H. Significant effects of powder preparation processes on the physical properties of  $\text{Bi}_{0.5}\text{Na}_{0.5}\text{TiO}_3\text{-}0.06\text{BaTiO}_3$  ceramic. *J Mater Sci Mater Electron.* 2014;25(12):5309-15.
- [49] Guo Y, Xiao P, Luo L, Jiang N, Lei F, Zheng Q, et al. Structure, ferroelectric and piezoelectric properties of  $\text{Bi}_{0.5}(\text{Na}_{0.8}\text{K}_{0.2})_{0.5}\text{TiO}_3$  modified  $\text{BiFeO}_3\text{-BaTiO}_3$  lead-free piezoelectric ceramics. *J Mater Sci Mater Electron.* 2014;25(9):3753-61.
- [50] Barick BK, Choudhary RN, Pradhan DK. Dielectric and impedance spectroscopy of zirconium modified  $(\text{Na}_{0.5}\text{Bi}_{0.5})\text{TiO}_3$  ceramics. *Ceram Int.* 2013;39(5):5695-704.
- [51] Behara S, Ghatti L, Kanthamani S, Dimpala M, Thomas T. Structural, optical, and Raman studies of Gd doped sodium bismuth titanate. *Ceram Int.* 2018;44(11):12118-24.
- [52] Ruth DEJ, Muneeswaran M, Giridharan NV, Sundarakannan B. Structural and electrical properties of bismuth magnesium titanate substituted lead-free sodium bismuth titanate ceramics. *J Mater Sci Mater Electron.* 2016; 27(7):7018-23.
- [53] Hiruma Y, Nagata H, Takenaka T. Thermal depoling process and piezoelectric properties of bismuth sodium titanate ceramics. *J Appl Phys.* 2009;105(8):084112.
- [54] Hajra S, Sahoo S, De M, Rout PK, Tewari HS, Choudhary RNP. Structural and electrical characteristics of barium modified bismuth-sodium titanate  $(\text{Bi}_{0.49}\text{Na}_{0.49}\text{Ba}_{0.02})\text{TiO}_3$ . *J Mater Sci Mater Electron.* 2017;29(2):1463-72.
- [55] Wang J, Zhou C, Li Q, Zeng W, Xu J, Chen G, et al. Dual relaxation behaviors and large electrostrictive properties of  $\text{Bi}_{0.5}\text{Na}_{0.5}\text{TiO}_3\text{-Sr}_{0.85}\text{Bi}_{0.1}\text{TiO}_3$  ceramics. *J Mater Sci.* 2018;53(6):8844-54.
- [56] Du H, Luo F, Qu S, Pei Z, Zhu D, Zhou W. Phase structure, microstructure, and electrical properties of bismuth modified potassium-sodium niobium lead-free ceramics. *J Appl Phys.* 2007;102(5):054102.
- [57] Babu MVG, Kader SA, Muneeswaran M, Giridharan NV, Padiyan DP, Sundarakannan B. Enhanced piezoelectric constant and remnant polarisation in K-compensated sodium potassium bismuth titanate. *Mater Lett.* 2015;146:81-3.
- [58] Hiruma Y, Yoshii K, Nagata H, Takenaka T. Investigation of phase transition temperatures on  $(\text{Bi}_{1/2}\text{Na}_{1/2})\text{TiO}_3\text{-}(\text{Bi}_{1/2}\text{K}_{1/2})\text{TiO}_3$  and  $(\text{Bi}_{1/2}\text{Na}_{1/2})\text{TiO}_3\text{-BaTiO}_3$  lead-free piezoelectric ceramics by electrical measurements. *Ferroelectrics.* 2007;346(1):114-9.

[59] Li S, Liu J, Guo T, Dong W, Bi K, Luo Y. Piezoelectricity and flexoelectricity of sodium bismuth titanate-based ceramics. *Ceram Int*. 2020;46:2049-54.

[60] Sahoo S, Hajra S, De M, Choudhary RN. Resistive, capacitive and conducting properties of  $\text{Bi}_{0.5}\text{Na}_{0.5}\text{TiO}_3\text{-BaTiO}_3$  solid solution. *Ceram Int*. 2018;44(5):4719-26.

[61] Yang M, Wang C, Peng Z, Fu X. Doping effect of  $\text{Ta}^{5+}$  ions on microstructure and electrical properties of  $\text{BaTiO}_3\text{-}(\text{Bi}_{0.5}\text{Na}_{0.5})\text{TiO}_3$  ceramics with positive temperature coefficient of resistivity. *J Mater Sci Mater Electron*. 2017;28(14):10589-95.

[62] Wang J, Zhang C, Wu F, Lin W, He X, Liu D, et al. Intrinsic and extrinsic electric response in  $\text{Bi}_{0.5}\text{Na}_{0.5}\text{TiO}_3\text{-BaTiO}_3$  lead-free piezoceramics. *Ferroelectrics*. 2019;547(1):156-63.

[63] Cernea M, Trupina L, Dragoi C, Galca AC, Trinca L. Structural, optical, and electric properties of BNT-BT<sub>0.08</sub> thin films processed by sol-gel technique. *J Mater Sci*. 2012;47(19):6966-71.

[64] Bajpai PK, Singh KN, Tamrakar P. Relaxor behavior and dielectric relaxation in lead-free solid solutions of (1-x)  $(\text{Bi}_{0.5}\text{Na}_{0.5}\text{TiO}_3)\text{-x}(\text{SrNb}_2\text{O}_6)$ . *J Electron Mater*. 2016;45:928-39.

[65] Anem S, Rao KS, Rao KH. Investigation of lanthanum substitution in lead-free BNBT ceramics for transducer applications. *Ceram Int*. 2016;42(14):15319-26.

[66] Sumang R, Kornphom C, Bongkarn T. Synthesis and electrical properties of BNT-BKT-KNN lead free piezoelectric solid solution prepared via the combustion technique. *Ferroelectrics*. 2017;518(1):11-22.

[67] Lu YQ, Li YX. A review on lead-free piezoelectric ceramics studies in China. *J Adv Dielectrics*. 2011;1(03):269-88.

[68] Sumang R, Thongmee N, Ketwong N, Sodnamorn P, Bongkarn T. Phase transition and electrical properties of [(0.935-x)BNT-0.065BT-xBZT] lead-free piezoelectric ceramics. *Ferroelectrics*. 2019;552(1):148-58.

[69] Moosavi A, Bahrevar MA, Aghaei AR, Castro A, Ramos P, Alguero M, et al. Effects of nano-sized  $\text{BiFeO}_3$  addition on the properties of high piezoelectric response (1-x)  $\text{Bi}_{0.5}\text{Na}_{0.5}\text{TiO}_3\text{-Bi}_{0.5}\text{K}_{0.5}\text{TiO}_3$  ceramics. *J Mater Sci*. 2015;50(5):2093-102.

[70] Zhou X, Yuan X, Yan Z, Xue G, Luo H, Zhang D. High piezoelectric response and excellent fatigue resistance in Rb-substituted BNT-BKT-BT ceramics. *J Mater Sci*. 2020;55(8):7634-44.

[71] Trelcat JF, Courtois C, Rguiti M, Leriche A, Duvigneaud PH, Segato T. Morphotropic phase boundary in the BNT-BT-BKT system. *Ceram Int*. 2012;38(4):2823-7.

[72] Xiao M, Sun H, Wei Y, Li L, Zhang P. Microstructure and dielectric properties of  $\text{BaTiO}_3\text{-}(\text{Bi}_{0.5}\text{Na}_{0.5})\text{TiO}_3\text{-NiNb}_2\text{O}_6$  ceramics. *J Mater Sci Mater Electron*. 2018;29(6):17689-94.

[73] Mohanty SK, Datta DP, Behera B, Mohanty HS, Pati B, Das PR. Synthesis and dielectric spectroscopic study of lead-free ferroelectric ceramic  $\text{K}_{0.5}\text{Bi}_{0.5}\text{TiO}_3\text{-NaNbO}_3$ . *J Mater Sci Mater Electron*. 2020;31(4):3245-55.

[74] Kang W, Zheng Z, Li Y, Zhao R. Enhanced dielectric and piezoelectric performance of sol-gel derived (1-x)  $\text{Bi}_{0.5}(\text{Na}_{0.78}\text{K}_{0.22})_{0.5}\text{TiO}_3\text{-xBaTiO}_3$  ceramics. *Ceram Int*. 2019;45(17):23078-83.

[75] Halim NA, Velayutham TS, Majid WA. Pyroelectric, ferroelectric, piezoelectric and dielectric properties of  $\text{Na}_{0.5}\text{Bi}_{0.5}\text{TiO}_3$  ceramic prepared by sol-gel method. *Ceram Int*. 2016;42(14):15664-70.

[76] Jaiban P, Jiamsirisomboon S, Watcharapasorn A, Yimnirun R, Guo R, Bhalla AS. High-and low-field dielectric responses and ferroelectric properties of  $(\text{Bi}_{0.5}\text{Na}_{0.5})\text{Zr}_{1-x}\text{TiO}_3$  ceramics. *Ceram Int*. 2013;39:S81-5.

[77] Hong CH, Kim HP, Choi BY, Han HS, Son JS, Ahn CW, et al. Lead-free piezoceramics-where to move on?. *J Materomics*. 2016;2(1):1-24.

[78] Zhang X, Liu Y, Yu Z, Lyu Y, Lyu C. Phase transition and huge field-induced strain of  $\text{BaZrO}_3$  modified  $(\text{Bi}_{0.5}\text{Na}_{0.5})_{0.94}\text{Ba}_{0.06}\text{TiO}_3$  ceramics. *J Mater Sci Mater Electron*. 2017;28:14664-71.

[79] Cheng R, Zhu L, Zhu Y, Xu Z, Chu R, Li H, et al. Giant piezoelectricity and ultrahigh strain response in bismuth sodium titanate lead-free ceramics. *Mater Lett*. 2016;165:143-6.

[80] Taghaddos E, Ma T, Zhong H, Zhou Q, Wan MX, Safari A. Fabrication and characterization of single-aperture 3.5-MHz BNT-based ultrasonic transducer for therapeutic application. *IEEE Trans Ultrason Ferroelectr Freq Control*. 2018;65(4):582-8.

[81] Taghaddos E, Hejazi M, Safari A. Lead-free piezoelectric materials and ultrasonic transducers for medical imaging. *J Adv Dielectrics*. 2015;5(2):1530002.

[82] Cernea M, Vasile BS, Ciuchi IV, Surdu VA, Bartha C, Iuga A, et al. Synthesis and characterization of novel ferrite-piezoelectric multiferroic core-shell-type structure. *J Mater Sci*. 2018;53(13):9650-61.

[83] Jaita P, Manotham S, Butnoin P, Sanjoom R, Arkornsakul P, Sweatman DR, et al. The mechanical and electrical properties of modified-BNKT lead-free ceramics. *Integrated Ferroelectrics Int J*. 2018;187(1):147-55.

[84] Kantha P, Pisitpipathsin N. Effect of  $\text{KNbO}_3$  addition on diffuse phase transition and dielectric properties of  $\text{Bi}_{0.5}\text{Na}_{0.5}\text{TiO}_3$  ceramics. *Integrated Ferroelectrics Int J*. 2018;187(1):129-37.

[85] Fernandez-Benavides DA, Gutierrez-Perez AI, Benitez-Castro AM, Ayala-Ayala MT, Moreno-Murguia B, Munoz-Saldana J. Comparative study of ferroelectric and piezoelectric properties of BNT-BKT-BT ceramics near the phase transition zone. *Materials*. 2018;11(3):361.

[86] Jeon YH, Patterson EA, Cann DP, Gibbons BJ. Dielectric and ferroelectric properties of  $(\text{Bi}_{0.5}\text{Na}_{0.5})\text{TiO}_3\text{-}(\text{Bi}_{0.5}\text{K}_{0.5})\text{TiO}_3\text{-BaTiO}_3$  thin films deposited via chemical solution deposition. *Mater Lett*. 2013;106:63-6.

[87] Christensen M, Einarsrud MA, Grande T. Fabrication of lead-free  $\text{Bi}_{0.5}\text{Na}_{0.5}\text{TiO}_3$  thin films by aqueous chemical solution deposition. *Materials*. 2017;10(3):213.

[88] Li J, Chen G, Lin X, Huang S, Cheng X. Enhanced energy density in poly(vinylidene fluoride) nanocomposites with dopamine-modified BNT nanoparticles. *J Mater Sci*. 2020;55(6):2503-15.

[89] Jeong CK. Toward bioimplantable and biocompatible flexible energy harvesters using piezoelectric ceramic materials. *MRS Communications*. 2020;10(3):365-78.

[90] Zhang Y, Kim H, Wang Q, Jo W, Kingon A, Kim S, et al. Progress in lead-free piezoelectric nanofiller materials and related composite nanogenerator devices. *Nanoscale Adv*. 2020;2(8):3131-49.

[91] Nanda D, Kumar P, Samanta B, Sahu R, Singh A. Structural, dielectric, ferroelectric and magnetic properties of (BNT-BT)-NCZF composites synthesized by a microwave-assisted solid-state reaction route. *J Electron Mater*. 2019;48(8):5039-47.

[92] Yao M, Pu Y, Zhang L, Chen M. Enhanced energy storage properties of (1-x)  $\text{Bi}_{0.5}\text{Na}_{0.5}\text{TiO}_3\text{-xBa}_{0.85}\text{Ca}_{0.15}\text{Ti}_{0.9}\text{Zr}_{0.1}\text{O}_3$  ceramics. *Mater Lett*. 2016;174:110-3.

[93] Pu Y, Yao M, Liu H, Fromling T. Phase transition behavior, dielectric and ferroelectric properties of (1-x)  $(\text{Bi}_{0.5}\text{Na}_{0.5})\text{TiO}_3\text{-xBa}_{0.85}\text{Ca}_{0.15}\text{Ti}_{0.9}\text{Zr}_{0.1}\text{O}_3$  ceramics. *J Eur Ceram Soc*. 2016;36(10):2461-8.

- [94] Fan P, Zhang Y, Huang J, Hu W, Huang D, Liu Z, et al. Constrained sintering and electrical properties of BNT-BKT lead-free piezoceramic thick films. *Ceram Int*. 2016;42(2):2534-41.
- [95] Aoyagi R, Takeda H, Okamura S, Shiosaki T. Ferroelectric and piezoelectric properties of bismuth layered-structure ferroelectric (Sr, Na, Bi)  $\text{Bi}_2\text{Ta}_2\text{O}_9$  ceramics. *Mater Sci Eng B*. 2005;116(2):156-60.
- [96] Badapanda T, Sahoo S, Nayak P. Dielectric, ferroelectric and piezoelectric study of BNT-BT solid solutions around the MPB region. *IOP Conf Mater Sci Eng*. 2017;178(1):012032.
- [97] Smolensky GA. New ferroelectrics of complex composition. IV. *Mater Sci*. 1961;2:2651-4.